Infrared ship signature analysis and optimisation

Filip Neele*
TNO Defence, Security and Safety, The Hague, The Netherlands

ABSTRACT

The last decade has seen an increase in the awareness of the infrared signature of naval ships. New ship designs show that infrared signature reduction measures are being incorporated, such as exhaust gas cooling systems, relocation of the exhausts and surface cooling systems. Hull and superstructure are cooled with dedicated spray systems, in addition to special paint systems that are being developed for optimum stealth. This paper presents a method to develop requirements for the emissivity of a ship's coating that reduces the contrast of the ship against its background in the wavelength band or bands of threat sensors. As this contrast strongly depends on the atmospheric environment, these requirements must follow from a detailed analysis of the infrared signature of the ship in its expected areas of operation. Weather statistics for a large number of areas have been collected to produce a series of 'standard environments'. These environments have been used to demonstrate the method of specifying coating emissivity requirements. Results are presented to show that the optimised coatings reduce the temperature contrast. The use of the standard environments yields a complete, yet concise, description of the signature of the ship over its areas of operation. The signature results illustrate the strong dependence of the infrared signature on the atmospheric environment and can be used to identify those conditions where signature reduction is most effective in reducing the ship's susceptibility to detection by IR sensors.

Keywords: Ships, infrared signature, signature prediction model, signature optimisation

1. INTRODUCTION

New ship designs show the impact of the increasing use of electro-optical observation and guiding sensors in threat systems. Following the advent of ship designs with a low radar cross section, infrared signature reduction techniques[1,2] have been incorporated in the latest designs. Exhaust pipes are being removed from the topside to the stern and exhaust gas cooling systems are installed. What remains for the infrared observation systems to detect is a hull and superstructure with few hotspots. The next step in the reduction of the infrared signature would be to apply a dedicated paint system, which matches the apparent temperature of the ship with the background. Unfortunately, the apparent temperature of both the ship and the background are strongly variable, with variations occurring on a time scale as short as minutes. If infrared signature reduction is to be obtained with standard coatings, then the optimum coating can only on average decrease the ship's signature, where the average is over the range of meteorological conditions the ship encounters in its areas of operation.

This paper presents a method to derive the optical properties of such an optimised coating. The method is based on the minimisation of the apparent temperature difference between ship and background using the spectral emissivity of the coating. The method is demonstrated for a simple ship model, for which the infrared signature is computed in a wide variety of environments. A set of environments is defined to encompass the variations in infrared signature of the ship in its areas of operation. This leads to a complete, but sufficiently concise description of the ship's signature. Optimised coatings are derived for several subsets of the complete set of environments and the signature reduction obtained with these coatings is demonstrated. This approach can be viewed as a step towards mission-specific coatings. Depending on the specific mission, the proper optimised coating could be applied on the ship immediately prior to the operations.

* filip.neele@tno.nl; phone +31 70 374 0461; fax +31 70 374 0654

Targets and Backgrounds XI: Characterization and Representation, edited by Wendell R. Watkins, Dieter Clement, William R. Reynolds, Proceedings of SPIE Vol. 5811
(SPIE, Bellingham, WA, 2005) · 0277-786X/05/$15 · doi: 10.1117/12.603404

2. METHOD

2.1 Ship model

A simple ship model is used in this study. The ship is represented by an element of the superstructure of a frigate-sized ship; it measures 10×20 m². This would be a typical element of a ship that appears above the horizon (ignoring distortion by mirage effects), which also applies to bow-on or stern-on views. The target is constructed of steel plates 1 cm thick (heat conductivity 80 W/m/K) and insulated with 15 cm of polystyrene foam (heat conductivity 0.8 W/m/K). The internal temperature of the target is 21 °C. The target surface is vertical, its normal is oriented at the horizon.

As a reference, temperature contrasts are first calculated for a target with a coating with spectral emissivity as shown in Figure 1. This paint is represents a typical mid-grey paint, with an emissivity near unity at infrared wavelengths. Further calculations with paints with different spectral emissivity are presented below.

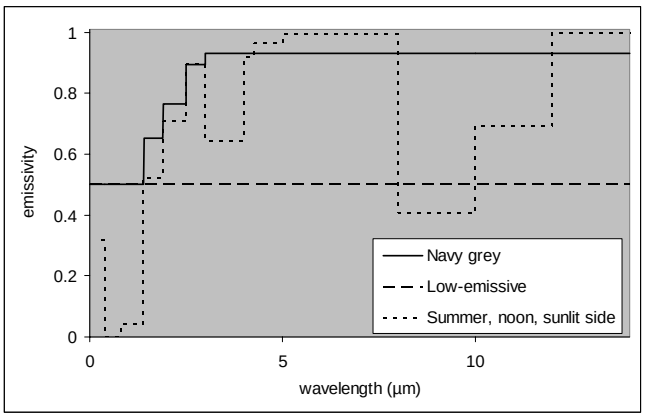

Figure 1. Solid curve: spectral emissivity of the paint applied to the target. At short wavelength the emissivity is 50%, while at infrared wavelengths the emissivity is near unity (93%). Dashed curve: hypothetical low-emissive paint, with an emissivity of 50% throughout the spectrum. Dotted curve: emissivity curve that minimises the temperature contrast of the sunlit side of targets, in both the 3-5 µm and 8-12 µm bands.

2.2 Atmospheric environment

As the infrared signature of ships, like that of any target, strongly depends on the atmospheric environment, a rigorous analysis of the infrared signature of any ship should encompass its behaviour in a wide range of environments. The expected operational areas of the ship should be the basis for an environment data base. This paper is not aimed at any existing ship and a list of environments is built by selecting five different geographical areas (North Sea, Mediterranean, sub-tropical, tropical and sub-arctic). To cover the extreme meteorological conditions, eight environments are defined in each area, by selecting the season (summer, winter), the time of day (noon, midnight), and weather type (clear sky, overcast). Table 1 lists the resulting 40 environments.

A database of sky radiance and solar irradiation was compiled for these environments. A world-wide database of meteorological observations in the period 1998-2002 provided the necessary input data for MODTRAN 4.0 (Table 2). Additional input data for MODTRAN were visibility (fixed at 15 km), cloud model parameters for overcast conditions (MODTRAN cloud model 4, with cloud base height at 1 km, cloud thickness of 1 km and extinction of 10 km^{-1}) and the vertical profiles of air temperature, relative humidity and pressure. These were copied from the standard atmospheric models (last column in Table 2), inserting air temperature, relative humidity and pressure at the lowest level in the profile. The solar zenith angle is given for noon and midnight, local time. Zenith angle is counted from zero at the zenith, through 90° at the horizon and 180° at nadir. At midnight, the solar zenith angle was set at 135°, which is well below the horizon. The solar azimuth was fixed at 180° (South) at noon.

2.3 Signature prediction code

Infrared signatures were computed with the signature prediction module EOSM in EOSTAR[3]. This module computes the heat flux balance for each facet of a multi-facet target, taking into account directional sky radiance, sea radiance, solar irradiation, convective flux to the ambient air and conduction to the interior. The code computes the fluxes in the spectral domain and outputs the spectral radiance of each facet in any desired part of the electro-optical spectrum. Facet radiance includes the reflected fractions of sea, sun and sky irradiation, as computed with MODTRAN[4]. The code has a BRDF capability, but that was not used here. The model has been extended with a dedicated optimisation algorithm, that computes the coating emissivity required to minimise the apparent temperature contrast in specified wavelength bands. This algorithm is described in section 2.4.

The signature prediction code has been validated with data from signature measurement trials on ships[5], as well as with data from scale models that were installed on top of a building and monitored for an extended period of time.

Table 1. List of environments used to represent a wide range of areas of operation. In each geographical area, several weather conditions in winter and summer are chosen to cover the average extreme conditions.

#	Region	Season	Weather	Time of day
1	North Sea	Summer (August)	Clear sky	Noon
2	North Sea	Summer (August)	Clear sky	Midnight
3	North Sea	Summer (August)	Overcast	Noon
4	North Sea	Summer (August)	Overcast	Midnight
5	North Sea	Winter (January)	Clear sky	Noon
6	North Sea	Winter (January)	Clear sky	Midnight
7	North Sea	Winter (January)	Overcast	Noon
8	North Sea	Winter (January)	Overcast	Midnight
9	Mediterranean	Summer (August)	Clear sky	Noon
10	Mediterranean	Summer (August)	Clear sky	Midnight
11	Mediterranean	Summer (August)	Overcast	Noon
12	Mediterranean	Summer (August)	Overcast	Midnight
13	Mediterranean	Winter (January)	Clear sky	Noon
14	Mediterranean	Winter (January)	Clear sky	Midnight
15	Mediterranean	Winter (January)	Overcast	Noon
16	Mediterranean	Winter (January)	Overcast	Midnight
17	Sub-tropical	Summer (August)	Clear sky	Noon
18	Sub-tropical	Summer (August)	Clear sky	Midnight
19	Sub-tropical	Summer (August)	Overcast	Noon
20	Sub-tropical	Summer (August)	Overcast	Midnight
21	Sub-tropical	Winter (January)	Clear sky	Noon
22	Sub-tropical	Winter (January)	Clear sky	Midnight
23	Sub-tropical	Winter (January)	Overcast	Noon
24	Sub-tropical	Winter (January)	Overcast	Midnight
25	Tropical	Summer (August)	Clear sky	Noon
26	Tropical	Summer (August)	Clear sky	Midnight
27	Tropical	Summer (August)	Overcast	Noon
28	Tropical	Summer (August)	Overcast	Midnight
29	Tropical	Winter (January)	Clear sky	Noon
30	Tropical	Winter (January)	Clear sky	Midnight
31	Tropical	Winter (January)	Overcast	Noon
32	Tropical	Winter (January)	Overcast	Midnight
33	Sub-arctic	Summer (August)	Clear sky	Noon
34	Sub-arctic	Summer (August)	Clear sky	Midnight
35	Sub-arctic	Summer (August)	Overcast	Noon
36	Sub-arctic	Summer (August)	Overcast	Midnight
37	Sub-arctic	Winter (January)	Clear sky	Noon
38	Sub-arctic	Winter (January)	Clear sky	Midnight
39	Sub-arctic	Winter (January)	Overcast	Noon
40	Sub-arctic	Winter (January)	Overcast	Midnight

Table 2. List of meteorological data for each of the environments of Table 1.

#	Julian day	T_{air} (K)	RH (%)	Pressure (mbar)	T_{sea} (K)	Solar zenith angle (°)	Latitude (°)	wind speed (m/s)	Modtran atmosphere #
1	228	290	80	1014	289	41	55	5.3	2
2	228	288	89	1015	289	135	55	5	2
3	228	290	80	1014	289	41	55	5.3	2
4	228	288	89	1015	289	135	55	5	2
5	15	279	83	1014	280	76	55	7.8	3
6	15	279	85	1013	280	135	55	8.2	3
7	15	279	83	1014	280	76	55	7.8	3
8	15	279	85	1013	280	135	55	8.2	3
9	228	302	74	1015	300	17	31	4.6	2
10	228	299	83	1015	300	135	31	4.9	2
11	228	302	74	1015	300	17	31	4.6	2
12	228	299	83	1015	300	135	31	4.9	2
13	15	290	67	1021	291	52	31	5.7	3
14	15	288	74	1021	291	135	31	5.5	3
15	15	290	67	1021	291	52	31	5.7	3
16	15	288	74	1021	291	135	31	5.5	3
17	228	303	78	1012	302	2	15	7.9	1
18	228	301	82	1012	302	135	15	8.1	1
19	228	303	78	1012	302	2	15	7.9	1
20	228	301	82	1012	302	135	15	8.1	1
21	15	301	77	1014	300	35	15	8.5	1
22	15	300	80	1014	300	135	15	8.4	1
23	15	301	77	1014	300	35	15	8.5	1
24	15	300	80	1014	300	135	15	8.4	1
25	228	311	51	998	306	15	28	3.9	1
26	228	307	68	998	306	135	28	4.2	1
27	228	311	51	998	306	15	28	3.9	1
28	228	307	68	998	306	135	28	4.2	1
29	15	292	65	1018	293	50	28	5.5	1
30	15	289	76	1018	293	135	28	5.2	1
31	15	292	65	1018	293	50	28	5.5	1
32	15	289	76	1018	293	135	28	5.2	1
33	228	287	83	1013	287	47	60	6.2	4
34	228	286	89	1013	287	135	60	6.2	4
35	228	287	83	1013	287	47	60	5.5	4
36	228	286	89	1013	287	135	60	5.2	4
37	15	280	80	1008	281	81	60	9.2	5
38	15	279	82	1008	281	135	60	9.4	5
39	15	280	80	1008	281	81	60	5.5	5
40	15	279	82	1008	281	135	60	5.2	5

2.4 Signature optimisation

In the sections below, the infrared signature optimisation is performed by adjusting the emissive properties of the coating to minimise the radiance contrast between target and background. The total emission of a target is the sum of self emission and reflected radiation from the environment, with (to first order) the coating emissivity as the trade-off parameter. In many cases, the contrast with background, which in this study is taken to be the sky just above the horizon, can be made smaller and even reduced to zero by adjusting the emissivity of the coating. The in-band emissivity directly affects the in-band contrast, but out-of-band emissivity can have a significant effect as well. For example, absorption of solar irradiation at short wavelengths increases the temperature of the target, which affects the contrast at long wavelengths.

The relation between emissivity and contrast is complex and non-linear and the optimum emissivity must be found with an iterative method. For a given emissivity curve (vector) $\vec{\varepsilon}$, the method presented in this paper minimised the apparent temperature contrast. In other words, the equation to be solved is

(1) $$F = \Delta L(\vec{\varepsilon}) = 0$$

where ΔL is the radiance contrast. The penalty function F is a vector of length $N \times M$: N environments and M threat bands in which the radiance contrast is computed and must be minimised. The radiance contrast in the threat band depends not only on the emissivity, as explicitly shown in (1). However, for clarity, all other parameters that influence target radiance have been left out.

In most cases, the relation between ΔL and emissivity is nearly linear. Therefore, the root of (1) is found by iteratively locating the root using a first-order series expansion of F**.** Let $\vec{\varepsilon}^{\,k}$ be the emissivity vector for the k^{th} iteration, then the expression to find the next approximation $\vec{\varepsilon}^{\,k+1} = \vec{\varepsilon}^{\,k-1} + \Delta\vec{\varepsilon}^{\,k}$ is

(2) $$\partial_j F_i(\vec{\varepsilon}^{\,k-1})\Delta\varepsilon_j^k = -F_i(\vec{\varepsilon}^{\,k-1})$$

where the index j corresponds to the K wavelength bands in which the emissivity is to be optimised. This expression is the result of applying the Newton-Raphson method to (1). Expression (2) leads to a matrix equation with $N \times M$ equations with K unknowns, which is solved using singular-value decomposition (SVD). After each SVD step, all values ε_j are restricted to the interval [0, 1]. This way the method is forced to utilise trade-offs between different parts of the spectrum, such as lower absorption in the short wavelengths versus lower emissivity at longer wavelengths or high emissivity at long wavelengths to maximise radiative heat loss. This iterative process is continued to convergence, which can be checked by measuring the total change to the emissivity vector. Fortunately, in most cases there is only a single root in (2), making it unlikely for the method to end up in a local minimum.

In this method the threat bands do not need to coincide with any of the K wavelength bands of the emissivity vector. In addition, the K wavelength bands (in which the emissivity is optimised) need not cover the complete electro-optical spectrum. Only in those bands where emissivity can be tailored with current technology needs the above method be applied. In addition, the restriction to the interval of physically realistic emissivity values [0, 1] could be further refined by using the interval of feasible emissivity values, again with current technology. This way the method will produce those results that are feasible and that will give the best possible signature reduction.

The choice of the K bands with which the emissivity function is represented obviously has influences on the result. If, for example, the emissivity in the 3-5 µm band is represented by a single value, a different result will be obtained than when the band is split up into multiple bands. In the latter case, the presence of the CO_2 absorption band can be taken into account, as well as the fact that the upper boundary of the solar spectrum is at 4 µm. The discretisation of the spectrum for the emissivity function, i.e., the value of K, does not affect the minimisation process, only the resolution with which the root of (1) is found.

The optimisation method can be applied to one or more threat bands simultaneously, giving the best emissivity curve for signature reduction in all threat bands. The method can also be applied to more than a single atmospheric environment, resulting in an emissivity curve that works best in the ensemble of environments.

The minimisation of (1) is currently performed without applying weights if multiple threat bands are used. The magnitude of the contrast, measured in W/m²/sr, depends on the wavelength, and a straightforward combination of, for example, visual and long-wavelength infrared threat bands may lead to an unbalanced result. A solution could be to normalise the contrasts in the threat bands.

2.5 Scenarios

Before infrared signatures can be computed, the set of parameters related to the sensor and the relative orientations of target and sensor must be defined. The sensor is defined to be a broad-band sensor, operating in the 3-5 µm (MWIR) or

8-12 µm (LWIR) bands. It is at a low elevation, observing the target against the sky just above the horizon. The target's orientation is relevant only for noon-time, clear-sky conditions. The target is facing South when the sunlit side is viewed, and facing North when its shadow side is observed. One scenario is defined for each environment, with the exception of noon-time, clear-sky environments, for which two scenarios are created: one in which the sunlit side of the target is viewed and one in which the shadow side is viewed. The result is a total of 50 scenarios that are listed in Table 3.

Table 3. Scenarios, based on the environments in Tables 1 and 2.

Scenario	Environment	Description	Scenario	Environment	Description
1	1	Day, clear sky, sunlit side	26	21	Day, clear sky, sunlit side
2	1	Day, clear sky, shadow side	27	21	Day, clear sky, shadow side
3	2	Night	28	22	Night
4	3	Day, overcast	29	23	Day, overcast
5	4	Night, overcast	30	24	Night, overcast
6	5	Day, clear sky, sunlit side	31	25	Day, clear sky, sunlit side
7	5	Day, clear sky, shadow side	32	25	Day, clear sky, shadow side
8	6	Night	33	26	Night
9	7	Day, overcast	34	27	Day, overcast
10	8	Night, overcast	35	28	Night, overcast
11	9	Day, clear sky, sunlit side	36	29	Day, clear sky, sunlit side
12	9	Day, clear sky, shadow side	37	29	Day, clear sky, shadow side
13	10	Night	38	30	Night
14	11	Day, overcast	39	31	Day, overcast
15	12	Night, overcast	40	32	Night, overcast
16	13	Day, clear sky, sunlit side	41	33	Day, clear sky, sunlit side
17	13	Day, clear sky, shadow side	42	33	Day, clear sky, shadow side
18	14	Night	43	34	Night
19	15	Day, overcast	44	35	Day, overcast
20	16	Night, overcast	45	36	Night, overcast
21	17	Day, clear sky, sunlit side	46	37	Day, clear sky, sunlit side
22	17	Day, clear sky, shadow side	47	37	Day, clear sky, shadow side
23	18	Night	48	38	Night
24	19	Day, overcast	49	39	Day, overcast
25	20	Night, overcast	50	40	Night, overcast

3. SIGNATURE OPTIMISATION

Signature results are presented in terms of apparent temperature contrasts of the target against the background. Apparent temperature is presented in two wavelength bands: 3-5 µm and 8-12 µm. The background is taken to be the sky just above the horizon, representative for a sensor observing the target from a low elevation. The apparent temperature of the background directly affects the contrast results. To avoid the possibly warm sky in the South (for low solar elevation) or the possibly cold sky in the North, the apparent temperature of the sky in the East is used as background in all scenarios.

3.1 Navy grey paint

Figure 2 shows the apparent temperature contrasts for the 50 scenarios, using the 'navy grey' paint system shown in Figure 1 (solid curves). The results have been separated into five groups: sunlit side, shadow side (both noon-time, clear-sky conditions), daytime overcast, clear skies at night and overcast conditions at night. As expected, the largest contrasts are found when viewing the sunlit side of the target, when contrasts up to 15 °C are found. The contrasts in all other cases vary between 2 and 9 °C. The contrasts in the LWIR band (Figure 3) show more variation, with contrasts up to 23 °C on the sunlit side and contrasts larger than 10 °C at night in some environments.

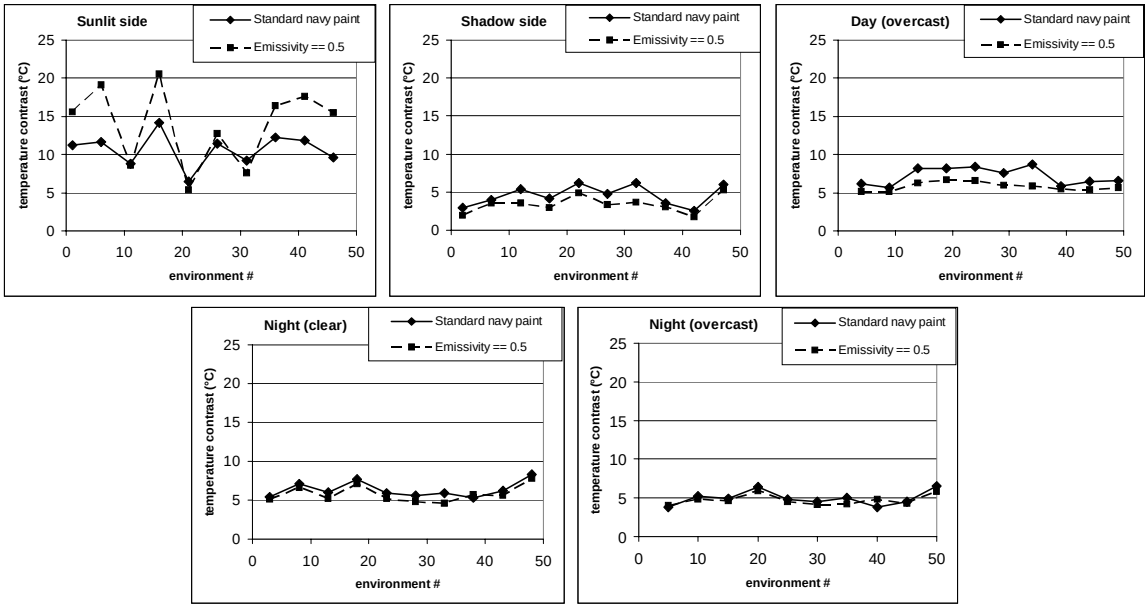

Figure 2. Temperature contrasts in the MWIR band. The results have been grouped into five categories: daytime clear-sky sunlit side, daytime clear-sky shadow side, daytime overcast sky; clear sky at night and overcast sky at night. In each frame, ten data points are shown, corresponding to the temperature contrast for the respective categories in summer and winter in the five areas of operation. Solid curve with diamonds: apparent temperature contrast for the standard navy paint. Dashed curve with squares: contrasts for the low-emissive paint. The emissivity curve for these paints is shown in Figure 1.

3.2 Optimised coatings: sunlit target

As a first step towards signature optimisation, Figures 2 and 3 also show the temperature contrasts obtained with the low-emissive paint shown by the dashed curve in Figure 1. This coating reduces the temperature contrast to a small extent in most scenarios in the MWIR band; the coating appears to be more effective in the LWIR band. In the MWIR band, this coating generally deteriorates the contrast of the sunlit side of the target. This is caused by a larger fraction of sunlight being reflected towards the sensor, which counters the effect of a possibly lower self-emission due to a lower temperature. This effect is smallest in those scenarios where the sun is at a high elevation: (sub-) tropical environments in the summer (scenarios 11, 21 and 31). In these scenarios direct solar irradiation of the target is low and the effects such as observed in scenarios 1, 6 and 16 are insignificant. In contrast, the low-emissive coating does produce good results in the LWIR band on the sunlit side of the target. In the absence of solar irradiation, the reduced emissivity reduces the apparent temperature contrast.

To demonstrate the signature optimisation method, an optimised emissivity curve is designed for the sunlit side of the target, in summer scenarios. As the temperature contrasts are largest for these scenarios, the effects of a dedicated coating should be evident. The optimisation was carried out for the MWIR and LWIR bands simultaneously. The electro-optical spectrum (0.3 – 40 µm) was divided into 25 bands, in which the emissivity was allowed to vary in the interval [0, 1]. For each of the five summer, noon-time sunlit side scenarios, an optimised coating was computed; the results were averaged to produce a single optimised coating. The resulting emissivity curve is shown in Figure 1 (dotted curve). The optimum coating for the sun side of the target has low emissivity – high reflectivity – at short wavelengths, resulting in low absorption of solar irradiation. This lowers the target temperature and decreases its apparent temperature at infrared wavelengths. In addition, the emissivity in the LWIR band is low, 0.4 – 0.7, to further decrease the apparent temperature of the target in that band. In the MWIR band, the sudden increase in emissivity at 4 µm coincides with the long-wavelength boundary of solar irradiation at sea level. Infrared emissivity is unity in those bands where no restriction are imposed on the contrast (5-8 µm, wavelengths longer than 12 µm); in these bands the target radiates its heat, rather than in the MWIR and LWIR bands. The low emissivity or, equivalently, the high reflectivity at short wavelengths results in a bright colour, which may increase the visual signature of the target during day time. Additional constraints could be put on the short-wavelength signature of the target, if necessary.

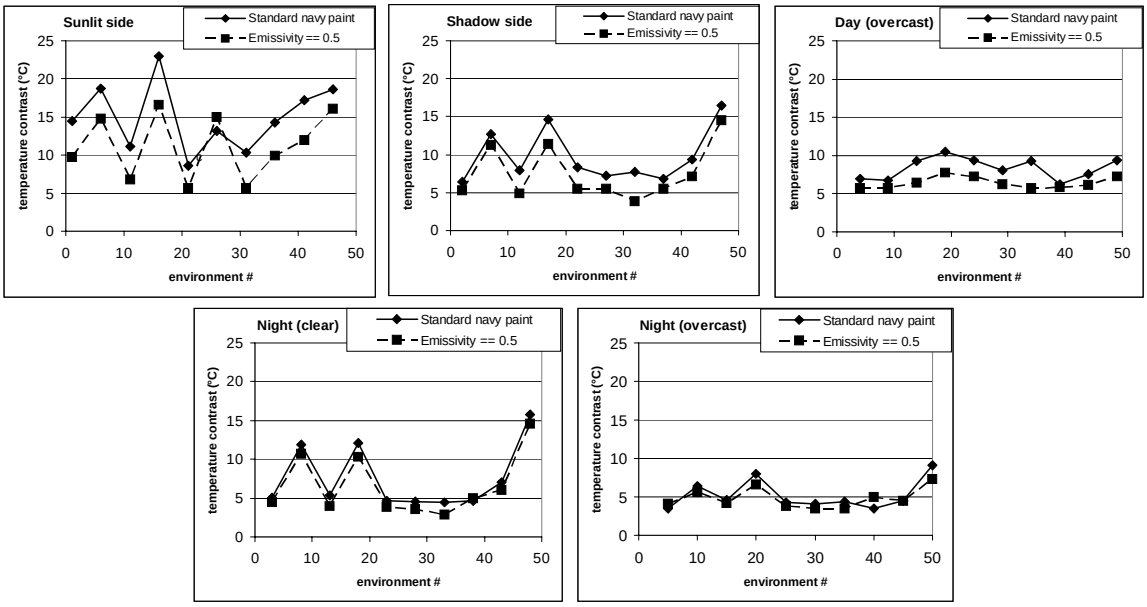

Figure 3. As Figure 2, showing results for the LWIR band.

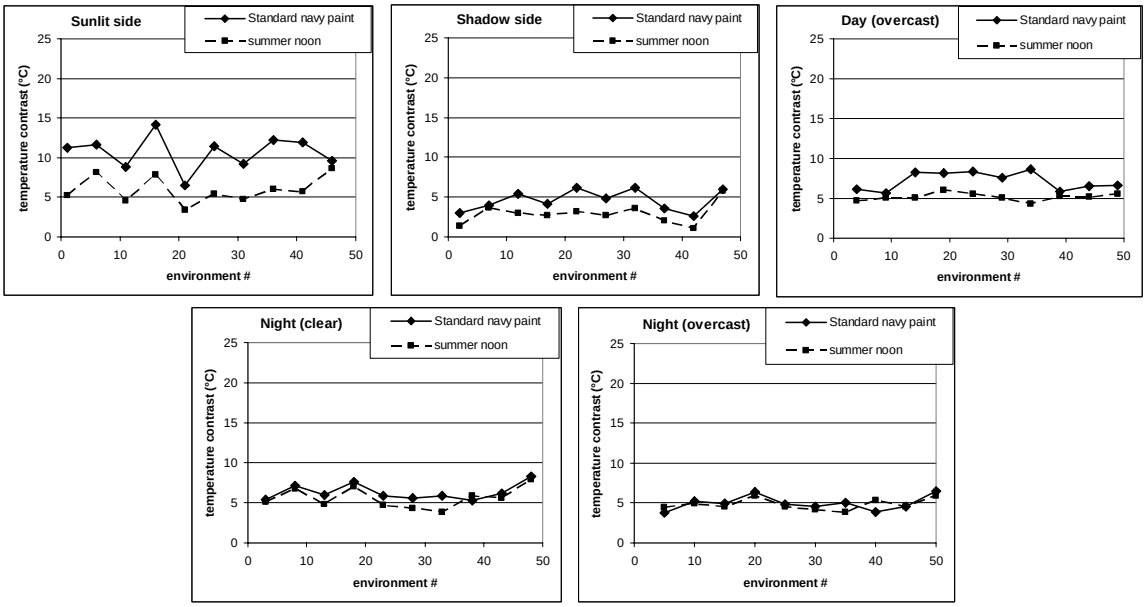

Figure 4. As Figure 2, comparing the signature results for the standard navy paint (solid curves, diamonds) with those for a paint optimised for summer, noon-time sunlit conditions (dashed curves, squares). Figure 1 shows the emissivity curve for the optimised paint.

Figure 4 shows the temperature contrasts obtained with this coating for the MWIR band. The temperature contrasts for the sunlit side in summer environments are about a factor of two smaller than with the standard navy grey coating. It is noted that the temperature contrasts of the sunlit side in winter environments (6, 16, 26, etc) have also improved. In addition, the temperature contrast of the shadow side and of the target in overcast conditions is also reduced by this coating, even though it was not designed for these environments. No or little improvement is observed in night time conditions. It is also noted that the optimised coating has a better performance than the simple low-emissive coating ($\varepsilon \equiv 0.5$). Although the latter coating also decreases temperature contrasts on the shadow side and in daytime overcast

conditions, it deteriorates the situation for the sunlit side. The optimised coating uses the spectral trade-offs in the heat balance fluxes, as discussed above, to decrease temperature contrast in all these scenarios.

Results for the LWIR band are shown in Figure 5. The optimised coating improved the signature of the sunlit side of the target, in both summer and winter conditions. With a few exceptions, the temperature contrast of the shadow side and of the target under overcast skies during daytime is below 5 °C. Again, no difference between the coatings is observed during the night.

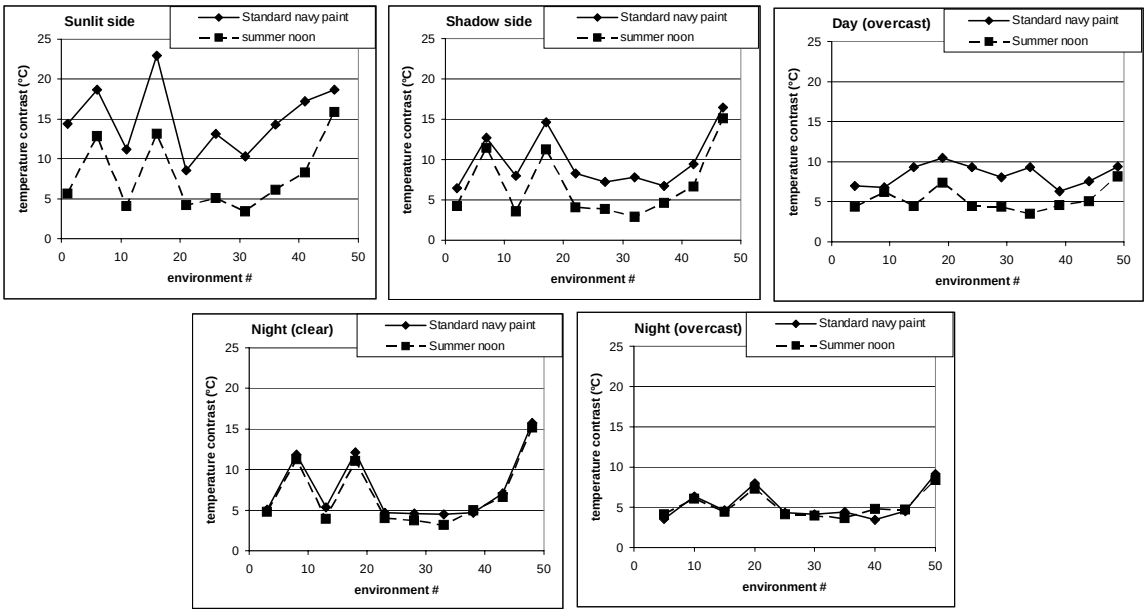

Figure 5. As Figure 4, now for the LWIR band.

3.3 Optimised coatings: other scenarios

The optimisation method was also applied to other subsets of the 50 scenarios. Figure 6 (left panel) shows the optimised coatings for the summer, clear-sky, noon, sunlit target side scenarios; this coating is the same as that shown in Figure 1. Figure 6 shows the average coating (thick curve), along with the standard deviation (thin curves), to show where the requirements for an optimised coating differ among the relevant scenarios. In this case, the requirements are similar and a single coating produces good results in all summer, clear-sky, noon, sunlit target side scenarios, as illustrated in Figure 4. The panel on the right-hand side in Figure 6 shows that an optimised coating for the shadow side in the same environments is only slightly different to that for the sunlit side, which explains the decreased apparent temperature contrasts for the shadow side in Figure 4.

Optimised coatings for winter environments are shown in Figure 7, again for the sunlit and shadow sides of the target. The emissivity curves are similar to those in Figure 6, but due to a lower elevation of the sun in winter, and lower temperature of the horizon background, the required emissivity in the MWIR and LWIR bands is lower. However, the differences are small and the performance in these scenarios of the optimised coating for summer scenarios is good (Figure 4), resulting in an overall reduction in apparent temperature contrast for both sunlit and shadow sides.

3.4 Optimised coatings: target orientation

As a final example, Figure 8 shows the dependence of the optimised coating on target orientation. Using again the summer, noon-time, clear-sky, sunlit side scenarios as starting point, optimised coatings were computed for target orientations between -20° and +20° from vertical. This range of orientations covers the majority of facet orientations on the superstructure of modern ships. The range of coatings that would be needed for a minimum average contrast is

typical of the range observed for the subsets used in Figure 7. It can be expected that a single coating would give good signature reduction results for hull and superstructure of a ship.

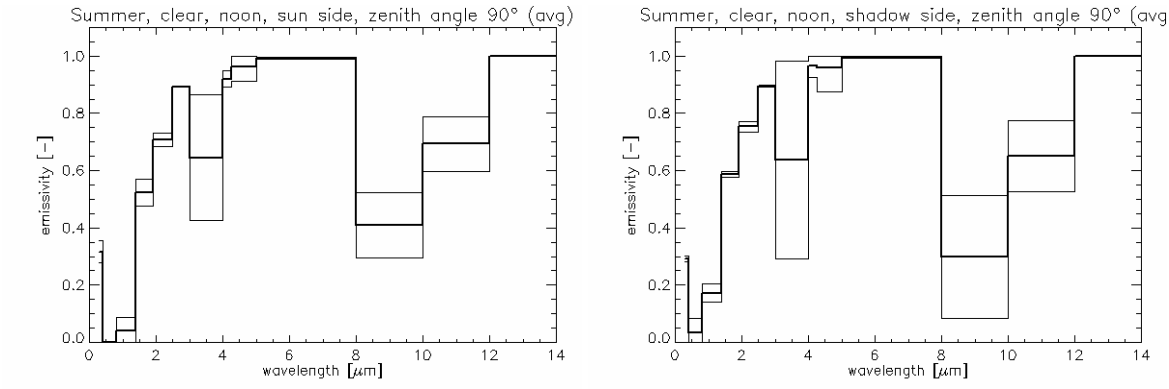

Figure 6. Optimised coatings. Each panel shows the optimised coating for a number of scenarios, with the solid curve representing the average and the thin curves at one standard deviation from the average. Left: scenarios summer, noon, sunlit side of target (same as dotted curve in Figure 1). Right: summer, noon, shadow side of target.

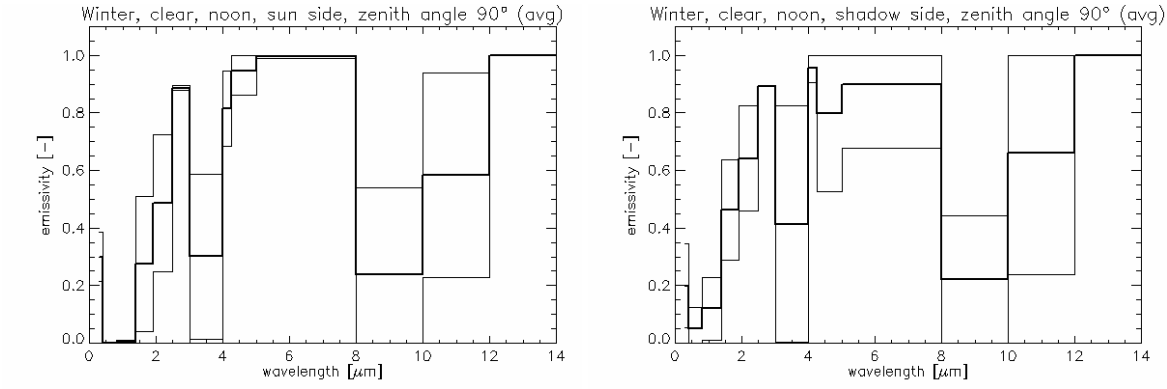

Figure 7. As Figure 6; left: scenarios winter, clear sky, noon, sunlit side; right: scenarios winter, clear sky, noon, shadow side

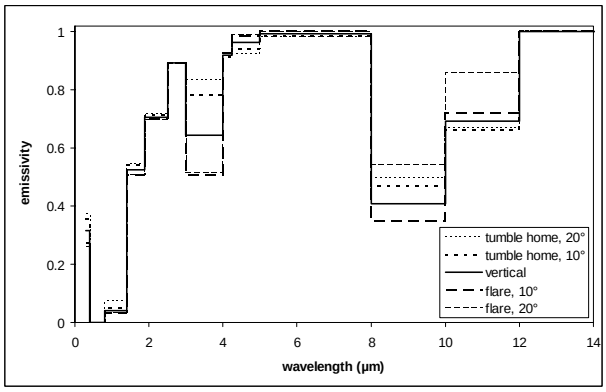

Figure 8. Dependence of the optimum coating emissivity on target orientation. The curves were computed for summer, clear-sky, sunlit side scenarios. Emissivity curves are shown for five orientations of the target, from -20° to +20° from vertical; ‘tumble home’ refers to target inclined towards the sky, while ‘flare’ refers to a target inclined towards the sea surface.

4. DISCUSSION

A method is presented for the optimisation of coating emissivity, to reduce the apparent temperature contrast of a ship's hull and superstructure with its background. The method minimises the contrast in any number of wavelength bands and in any number of scenarios. The performance of the method is illustrated by comparing the apparent temperature contrast in the mid-wave and long-wave infrared for a simple ship model, in a large number of atmospheric environments. The method provides the basis for a detailed analysis of the signature reduction that can be obtained by adjusting the optical properties of a ship's coating. Information about technically feasible spectral emissivity can be used to constrain the method, thus forcing the method to find the best possible coating that can be produced with current technology. Such information has not been used in this paper – which has probably resulted in emissivity curves that are not feasible with current technology – but this would be a logical next step.

The derivation of several optimised coatings, each for a different subset of the complete set of scenarios, could be viewed as the first step towards the use of mission-specific coatings. Such a coating would be applied on a ship, immediately prior to performing its missions, changing coatings as missions or area of operation changes.

A further step would be to adapt or optimise the direction-dependent reflection characteristics of a coating, by which means the reflection of irradiation from sea, sky and sun towards an observer can be tuned.

The analysis presented here is based on a set of environments, representing the areas of operation of the ship. Such an analysis is essential, as the infrared signature of ships, as of any object, varies with the conditions of the atmospheric environment. A relatively simple description of typical atmospheric conditions in a small number of operational areas already leads to a set of 50 scenarios in which the infrared signature is computed. The advantage of this approach is that the results give an impression of the performance of ship or ship design and highlight the areas where signature reduction is most effective.

To conclude, the results presented here constitute only part of a complete analysis of signature reduction. Signature reduction requirements should follow from operational requirements imposed on the ship. Whether or not the signature reduction provided by the optical properties of any given coating are sufficient must be judged from an operational analysis of the ship with the coating applied. This report provides a method to derive the optical properties of the coating and gives a description of how a set of reference environments can be set up.

5. ACKNOWLEDGEMENTS

This work has been done under contracts from the Royal Netherlands Navy. The work has benefited from discussions with Keith Youern (Dstl, UK).

REFERENCES

1. Neele, F.P. and W. de Jong, *Prewetting systems as an IR signature control tool*, SPIE Proc. 4718: Targets and backgrounds VIII: characterisation and representation, p. 156-163, SPIE, Orlando, 2002.
2. Schleijpen, H.M.A. and F.P. Neele, *Ship exhaust plume cooling*, SPIE Proc. 5431: Targets and backgrounds X: characterisation and representation, p. 66-76, SPIE, Orlando, 2004.
3. Kunz, G.K., M.A.C. Degache, M.M. Moerman, A.M.J. van Eijk, F.P. Neele, S.M. Doss-Hammel and D. Tsintikidis, *Status and developments in EOSTAR, a model to predict IR sensor performance in the marine environment*, SPIE's 11th International Symposium on Remote Sensing, 'Optics in Atmospheric Propagation and Adaptive Systems VII', Maspalomas, Gran Canaria, September 2004.
4. MODTRAN Air Force Research Laboratory web site: http://www.vs.afrl.af.mil/Division/VSBYB/modtran4.html.
5. Neele, F.P., *Infrared ship signature prediction, model validation and sky radiance*, SPIE Proc. 5811: Targets and backgrounds XI: characterization and representation, this volume, 2005.